Journal of Colloid and Interface Science 455 (2015) 46–54

Contents lists available at ScienceDirect

Journal of Colloid and Interface Science

www.elsevier.com/locate/jcis

General electrokinetic model for concentrated suspensions in aqueous electrolyte solutions: Electrophoretic mobility and electrical conductivity in static electric fields

Félix Carrique [a,*], Emilio Ruiz-Reina [b], Rafael Roa [c], Francisco J. Arroyo [d], Ángel V. Delgado [e]

[a] Departamento de Física Aplicada I, Facultad de Ciencias, Universidad de Málaga, 29071 Málaga, Spain
[b] Departamento de Física Aplicada II, Escuela Politécnica Superior, Universidad de Málaga, 29071 Málaga, Spain
[c] Forschungszentrum Jülich, Institute of Complex Systems (ICS-3), 52425 Jülich, Germany
[d] Departamento de Física, Facultad de Ciencias Experimentales, Universidad de Jaén, 23071 Jaén, Spain
[e] Departamento de Física Aplicada, Facultad de Ciencias, Universidad de Granada, 18071 Granada, Spain

GRAPHICAL ABSTRACT

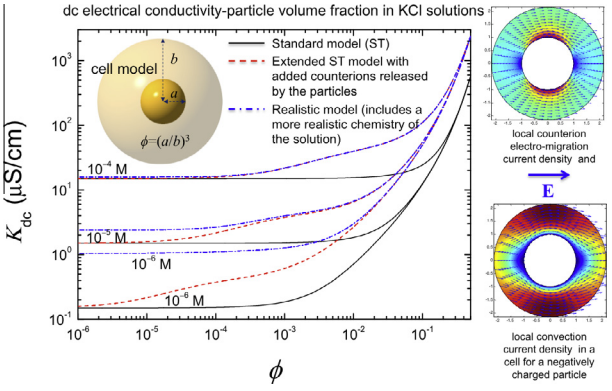

ARTICLE INFO

Article history:
Received 17 February 2015
Accepted 12 May 2015
Available online 16 May 2015

Keywords:
Concentrated suspensions
Cell model
Electrophoretic mobility
Electrical conductivity
Standard electrokinetic model
Aqueous electrolyte solutions

ABSTRACT

In recent years different electrokinetic cell models for concentrated colloidal suspensions in aqueous electrolyte solutions have been developed. They share some of its premises with the standard electrokinetic model for dilute colloidal suspensions, in particular, neglecting both the specific role of the so-called *added* counterions (i.e., those released by the particles to the solution as they get charged), and the realistic chemistry of the aqueous solution on such electrokinetic phenomena as electrophoresis and electrical conductivity. These assumptions, while having been accepted for dilute conditions (volume fractions of solids well below 1%, say), are now questioned when dealing with concentrated suspensions. In this work, we present a general electrokinetic cell model for such kind of systems, including the mentioned effects, and we also carry out a comparative study with the standard treatment (the standard solution only contains the ions that one purposely adds, without ionic contributions from particle charging or water chemistry). We also consider an intermediate model that neglects the realistic aqueous chemistry of the solution but accounts for the correct contribution of the added counterions. The results show the limits of applicability of the classical assumptions and allow one to better understand the relative role of the added counterions and ions stemming from the electrolyte in a realistic aqueous solution, on electrokinetic properties. For example, at low salt concentrations the realistic effects of the aqueous solution are the dominant ones, while as salt concentration is increased, it is this that progressively takes the

* Corresponding author.
E-mail address: carrique@uma.es (F. Carrique).

http://dx.doi.org/10.1016/j.jcis.2015.05.023

control of the electrokinetic response for low to moderate volume fractions. As expected, if the solids concentration is high enough the added counterions will play the dominant role (more important the higher the particle surface charge), no matter the salt concentration if it is not too high. We hope this work can help in setting up the real limits of applicability of the standard cell model for concentrated suspensions by a quantitative analysis of the different effects that have been classically disregarded, showing that in many cases they can be determinant to get rigorous predictions.

1. Introduction

The use of nanoparticle-based systems has experienced an outstanding increase in recent years, not only because of the many new physical phenomena unraveled by size reduction down to the nm scale, but also due to the growing number of technological and biomedical applications [1–3]. Although dilute suspensions of nanoparticles suspended in aqueous media have been extensively dealt with, it is the more practical use of the concentrated ones that has determined the present interest in their study.

In addition to different microscopies, electrokinetic techniques, especially electrophoresis, have proved to be very powerful in characterizing nanoparticles in suspension, mostly (but not only) in aqueous solutions [4]. In the last decades, models of electrophoresis for concentrated suspensions in the presence of *dc* or *ac* electric fields have been developed based on the cell model concept to account for particle–particle electrohydrodynamic interactions under a mean-field approach. An interested reader can find an extensive discussion about the cell model approach in the review by Zholkovskij et al. [5].

Closely related to the main topic of this contribution is the field of the so-called *salt free* suspension. Ideally, it is a suspension fully devoid of ions other than the "added" counterions, i.e., the countercharge released by the particles to the solution as they get charged. Salt-free suspensions have a special importance in soft matter physics especially in the process of formation of colloidal crystals, as long-range electrostatic interparticle interactions are less screened in such systems [6–10]. In the present study the suspensions also include an external salt, and we will be mainly concerned in exploring the role of the added counterions against those of the ionic species of the salt.

Interestingly, both aspects (volume fraction of dispersed solids) and low ion concentration are interrelated in situations where closely packed, typically spherical particles are investigated. In such cases, volume fractions of solids associated to the onset of crystallization range around and above 50%, whereas electrolyte concentrations are typically kept very low, in the vicinity of 1 μmol/L [11]. These would be typical situations in which the full model described in this paper can (and probably should) be used.

After the original contributions of Oosawa and collaborators [12] regarding the electrokinetics of dilute salt-free systems, Ohshima studied more recently several equilibrium and transport properties of these systems [13–17]. Later, Chiang et al. [18] extended the electrophoretic studies with salt-free suspensions to concentrated ones, and the present authors also contributed with electrokinetic [19] and rheological [20] models for these salt-free suspensions. Likewise, finite ion size effects have been added in order to achieve a quite complete description of concentrated salt-free suspensions [21].

A further model improvement was done by considering, what can be denominated realistic conditions in the chemistry of ionic species in aqueous solution, assuming in all cases equilibrium in all chemical reactions involved [22]. A more realistic model considers the role of ions coming from water dissociation and from the chemistry of possible carbon dioxide contamination of the solution under a non-equilibrium chemical approach for chemical reactions. The choice of a non-equilibrium scenario for chemical reactions obeys to the fact that forward and backward chemical reactions do not proceed necessarily at the same rate under the influence of external electric fields.

Results from new models for the above mentioned realistic salt-free suspensions have shown the importance of considering non-equilibrium association-dissociation chemical reactions in solution for a precise description of the electrokinetics of these systems [23]. Suffice it to mention that such models have been able to explain the presence of a low frequency relaxation process that had not been captured by previous theories based on the assumption of chemical equilibrium.

Many of the findings attained with realistic concentrated salt-free suspensions will be of worth for the development of the new model that includes an electrolyte in the solution. One can now wonder how far the predictions of such complete model may be from the classical or standard description of the electrokinetic response of dilute or concentrated suspensions in aqueous electrolyte solutions. There exist classical or standard models that predict that response. To begin with, these models [24–35] do not take into account the realistic chemistry of the aqueous solutions or the role of the (added) counterions released by the particles. For dilute suspensions and common electrolyte concentrations in solution, the latter two aspects have been historically underestimated or simply neglected, because of their admitted minor role in comparison with that of the salt. But nowadays, very highly charged concentrated suspensions in aqueous solutions can be developed in laboratories and industries. One such case is that of ceramic slurries: stable concentrated dispersions with particles bearing a high surface charge (either pH- or additive-dependent) produce the best green-body properties [36,37], and the same applies to pigments and paper fillers or coatings [38,39], or pharmaceutical suspensions [40,41], very often used with solids loads well above 20%. In all these instances it is mandatory to revise the influence of the latter simplifications as well as their limits of applicability.

Another complicating issue when dealing with highly charged particles is the phenomenon of the condensation of counterions that takes place in a region very close to the particles surface, playing a relevant role in the overall electrokinetic response. In fact, it has outstanding effects in the general electrostatics of soft matter, affecting the stability of colloids [42,43], or the self-assembly of biomolecules [44], as well as the compaction of genetic material [45]. The phenomenon also occurs in pure salt-free or low-salt regimes at finite volume fractions [46], and it has provided explanation to such findings as the independence of electrokinetic properties like electrophoretic mobility with particle charge [13–15,19], or the presence of a relaxation process linked to this condensate region in radiofrequency electric fields [23].

A complete model of the electrokinetics of these systems, considering the mathematical complexities involved, should only be used when the system truly requires it. Many situations might arise, depending on the nature of salt and the rest of ionic species in a realistic scenario, mainly that of the added counterions, in

which it would appear reasonable that all these aspects will decrease in relevance upon increasing the external salt concentration. In such conditions it would then be expected that the standard electrokinetic predictions, which only account for the charged particles and the external salt, tend to approach the predictions of the more sophisticated model we are concerned here. Thus, it would be of worth to properly establish the realm of standard models in predicting the electrokinetic response of a suspension in general electrolyte solutions. To that end, a rigorous comparison between new and standard predictions for many typical situations has been carried out in this work. We hope the present study will help in establishing the limits of the standard models to be used with guarantee in predicting the average electrokinetic response of a concentrated suspension in general electrolytes, or alternatively, to set the conditions under which the more general model developed in this work has to be used instead. Specifically, it will be found that the effect of added counterions is most important for moderate volume fractions of solids, whereas the specific chemistry of the solutions must be considered carefully if the suspension does not contain additional salt in solution, or if the concentration of the latter is close to or below 10^{-5} mol/L.

In this work, standard model results, full non-equilibrium ones and those obtained with a less stringent model with intermediate complexity will be presented and discussed for comparison. In order to avoid the analysis of the many different couplings than can arise when an external salt is added to the system, we will focus our attention only on concentrated suspensions in which the added counterions are H^+ if the particles are negatively charged, or OH^-, if positively charged. To this suspension an external salt will be added admitting that in solution it will be completely dissociated. Typical examples of such suspensions might be negatively charged polystyrene sulphonate latexes whose original counterions have been dialyzed against H^+. The medium will hence contain H^+ ions from the particle charging, the water dissociation and the dissociation of the carbonic acid H_2CO_3 generated by dissolved CO_2. Anions from the aqueous solution will be OH^-, HCO_3^-, and an externally added electrolyte, like KCl in the present study, will provide K^+ and Cl^-, ions. The electrokinetic response of this suspension in the presence of a static electric field (*dc* response) will be studied in terms of both, the particle electrophoretic mobility and the electrical conductivity of the suspension for many different conditions of particles and electrolyte solution.

2. Models to be compared

In the Supplementary Information file we have included a detailed account of the fundamentals of the possible descriptions of the electrokinetics of concentrated suspensions in electrolyte solutions, taking also into consideration the chemistry of water and dissolved CO_2 (FNEQ model, hereafter). In all cases, the finite concentration of particles will be taken into account following the Kuwabara cell model [47]: the suspension properties can be extracted from a single cell composed of a particle (spherical in our case, of radius a) located at the center of a sphere of solution of radius b. By applying proper boundary conditions at the cell boundary, it is supposed that the electro-hydrodynamic particle–particle interactions can be managed. This would be more plausible in homogeneous and isotropic suspensions. The size of the cell is obtained by forcing the particle volume fraction of the cell to coincide with the particle volume fraction ϕ of the whole suspension, that is, $\phi = (a/b)^3$. The particle is characterized by a surface charge density σ and the solution, with mass density ρ_s, viscosity η_s and relative permittivity ε_{rs}, will contain added counterions that will be assumed to be H^+, with valence $z_1 = +1$ and diffusion coefficient $D_1 = 9.3 \times 10^{-9}\ m^2\ s^{-1}$. The other species present are: OH^- ($z_2 = -1$, $D_2 = 5.3 \times 10^{-9}\ m^2\ s^{-1}$), HCO_3^- ($z_3 = -1$, $D_3 = 1.2 \times 10^{-9}\ m^2\ s^{-1}$), neutral H_2CO_3 (the solution is saturated with CO_2), with $z_4 = 0$ and $D_4 = 1.3 \times 10^{-9}\ m^2\ s^{-1}$ (estimated from Stokes law and using 0.18 nm as molecular size [48]), and of course H_2O and dissolved CO_2 being the concentration of the latter 1.08×10^{-5} M, calculated from its solubility and partial pressure in standard air at room temperature. The non-equilibrium association–dissociation processes for the chemical reactions in solution are:

$$\begin{aligned} &H_2O \underset{K_{-1}}{\overset{K_1}{\rightleftharpoons}} H^+ + OH^- \\ &H_2CO_3 \underset{K_{-2}}{\overset{K_2}{\rightleftharpoons}} H^+ + HCO_3^- \\ &H_2CO_3 \underset{K_{-3}}{\overset{K_3}{\rightleftharpoons}} CO_2 + H_2O \end{aligned} \tag{1}$$

where K_i and K_{-i} ($i = 1, 2, 3$) are forward (s^{-1}) and backward ($m^3 s^{-1}$) kinetic constants. The further dissociation of the bicarbonate anion HCO_3^- to give H^+ and $CO_3^=$ has been disregarded due to its minor quantitative role in the phenomena we are concerned with [22]. A salt is also added to the solution, KCl in this study, introducing in the problem two new ionic species K^+ ($z_5 = +1$, $D_5 = 1.9 \times 10^{-9}\ m^2\ s^{-1}$) and Cl^- ($z_6 = -1$, $D_6 = 2.0 \times 10^{-9}\ m^2\ s^{-1}$).

After the application to the suspension of an electric field $\mathbf{E}$, each particle will attain a steady state electrophoretic velocity $\mathbf{v}_e = \mu\mathbf{E}$, μ being the electrophoretic mobility. The reference system is fixed to the particle center, and spherical coordinates (r, θ, φ) will be used where the z axis ($\theta = 0$) is chosen parallel to the external electric field. It has been shown that due to the symmetry, some radial functions $h(r)$, $Y(r)$ and $\phi_j(r)$ can be defined containing information about the field-induced linear perturbations (the only ones considered in the present study) in the fluid velocity $\mathbf{v}$, the electric potential Ψ, and the electrochemical potential of j-th species μ_j, respectively [13,23]. The perturbation scheme is expressed as:

$$\mathbf{v}(\mathbf{r}) = (v_r, v_\theta, v_\varphi) = \left(-\frac{2}{r}hE\cos\theta,\ \frac{1}{r}\frac{d}{dr}(rh)E\sin\theta,\ 0\right) \tag{2}$$

$$\begin{aligned} &\Psi(\mathbf{r}) = \Psi^0(r) + \delta\Psi(\mathbf{r}) \\ &\delta\Psi(\mathbf{r}) = -Y(r)E\cos\theta \end{aligned} \tag{3}$$

$$\begin{aligned} &\mu_j(\mathbf{r}) = \mu_j^0 + \delta\mu_j(\mathbf{r}) \quad (j = 1, \ldots, 6) \\ &\delta\mu_j(\mathbf{r}) = z_j e\delta\Psi + k_B T\frac{\delta n_j}{n_j^0} = -z_j e\phi_j(r)E\cos\theta \quad (j = 1-3, 5-6) \\ &\delta\mu_{H_2CO_3}(\mathbf{r}) = -e\phi_{H_2CO_3}(r)E\cos\theta \quad (j = 4, H_2CO_3) \end{aligned} \tag{4}$$

$$P(\mathbf{r}, t) = P^0 + P(\mathbf{r}) \tag{5}$$

Here $E = |\mathbf{E}|$, n_j is the concentration in number of the j-th species, P is the pressure at every point $\mathbf{r}$ in the system, k_B is the Boltzmann constant and T and e the absolute temperature and the elementary electric charge, respectively. The "0" superscript refers to equilibrium quantities, and the field-induced perturbation of a given quantity X is expressed by δX. By way of example, Poisson equation (S1.1,2) transforms after substitution of Eqs. (3) and (4) as follows:

$$\begin{aligned} &\nabla^2\Psi(\mathbf{r}) = \nabla^2[\Psi^0(r) - Y(r)E\cos\theta] = \nabla^2\Psi^0(r) - E\cos\theta\ L[Y(r)] \\ &\rho_{el}(\mathbf{r}) = \sum_{k=1}^{n\_ions} z_k e[n_k^0(r) + \delta n_k(\mathbf{r})] = \rho_{el}^0(\mathbf{r}) \\ &\qquad + \sum_{k=1}^{n\_ions}\frac{z_k e}{k_B T}[-z_k e\phi_k(r)E\cos\theta - z_k e\delta\Psi(\mathbf{r})] \end{aligned} \tag{6}$$

Taking into account that $\nabla^2\Psi^0(r) = -\rho^0_{el}(\mathbf{r})/\varepsilon_{rs}\varepsilon_0$, and making use of the linear operator L defined in Eqs. (S1.19) and (S1.17) is obtained easily.

As was recently pointed out, in the non-equilibrium scenario that we also assume in the present model, the following conservation equations for all the ionic species linked by chemical reactions apply:

$$\nabla\cdot[n_j(\mathbf{r})\mathbf{v}_j(\mathbf{r})] = \sigma_j(\mathbf{r}), \quad (j=1,\ldots,4) \tag{7}$$

where the functions σ_j represent generation-recombination terms associated to the production or annihilation of ions by chemical reactions in the aqueous solution, expressed as in Eq. (S1.9), being $\mathbf{v}_j$ the drift velocity of the j-th species.

As usual, the ions coming from the external salt verify the continuity equations:

$$\nabla\cdot[n_j(\mathbf{r})\mathbf{v}_j(\mathbf{r})] = 0, \quad (j=5,6) \tag{8}$$

In this work, most of the theoretical results obtained from three models will be compared. All of them previously require the resolution of the Poisson–Boltzmann equation (PB) for the equilibrium double layer. In Section S3 of the Supplementary Information we provide details on the resolution of the PB equation applied in this paper.

The first of the models, that will be called ST (see Section S4), is the *standard electrokinetic cell model* for concentrated suspensions, based on the Shilov–Zharkikh–Borkovskaya boundary conditions [32,34] and its numerical resolution for arbitrary conditions. Even in this approach, there remain doubts as to what is the meaning of $n^{\infty}_{+,-}$ (Eq. S4.5) in the PB equation for concentrated suspensions. For the case of dilute suspensions the coefficients $n^{\infty}_{+,-}$ represent the ionic concentrations of the classical neutral bulk of the solution where supposedly the electrical potential is zero. But as discussed in S4, no clear bulk is found in many situations, and even more, it might not be attained in any place of the suspension because of the overlap of the double layers of neighbor particles. For the general model presented in this paper, differences can be found in the predictions of electrokinetic properties depending on the choice of the average salt concentration, mainly at high particle volume fractions. Of course, if we are concerned with comparing theoretical predictions and experimental data, it is quite important that any average salt concentration value be unambiguously fixed: it must be established whether the experimental average salt concentration corresponds to moles per unit suspension volume or moles per unit liquid volume part of the suspension. Once this aspect is made clear, the model will properly manage such choice to calculate the corresponding electrokinetic properties for comparison.

Finally, we will also check an intermediate model (AC + S model) which does not include any realistic chemistry of the solution and only considers in addition to the charged particles, their added counterions (AC) and the externally added salt (S) in the solution.

3. Results and discussion

3.1. Effects of the average salt concentration choice on local equilibrium ionic concentrations and electrokinetic properties in static electric fields

Before comparing the three models and, particularly, the effect that the realistic chemistry of the FNEQ approach has on electrokinetic properties, we will briefly consider the effect of the average concentration choice, that is, either referred to the full suspension volume (S), or just to its liquid part (l). In order to compare with the standard model (ST) predictions, the input reference molar concentrations ($c^{\infty}_{+,-}$) will be taken as identical to the nominal values of $c_{+,-l}$ or $c_{+,-S}$.

In Fig. 1a we show the dimensionless electrophoretic mobility (Eq. S1.41)-volume fraction predictions for AC + S (l), AC + S (S) and ST models for the lowest particle surface charge density studied $\sigma = -0.05$ μC/cm^2. Mobility data for highly charged particles are displayed in Fig. 2a. The same kind of calculations, regarding the dc conductivity, are plotted in Figs. 1b and 2b. Some interesting features can be drawn of these figures. Let us start with the case of the lowest particle surface charge density in Fig. 1a and b:

(i) As expected, and in general terms, the discrepancies between AC + S (l) and AC + S (S) predictions are relatively more important at high volume fractions and high electrolyte concentrations (the effect is more evident for the *dc* conductivity in Fig. 1b).

(ii) At very low salt concentrations both AC + S predictions tend to coincide whatever the volume fraction because of the minor role of the salt ions against that of the added counterions at such conditions.

(iii) ST predictions deviate more from either AC + S (S) or AC + S (l) ones the lower the salt concentration because of the increasing importance of the added counterions in low-salt

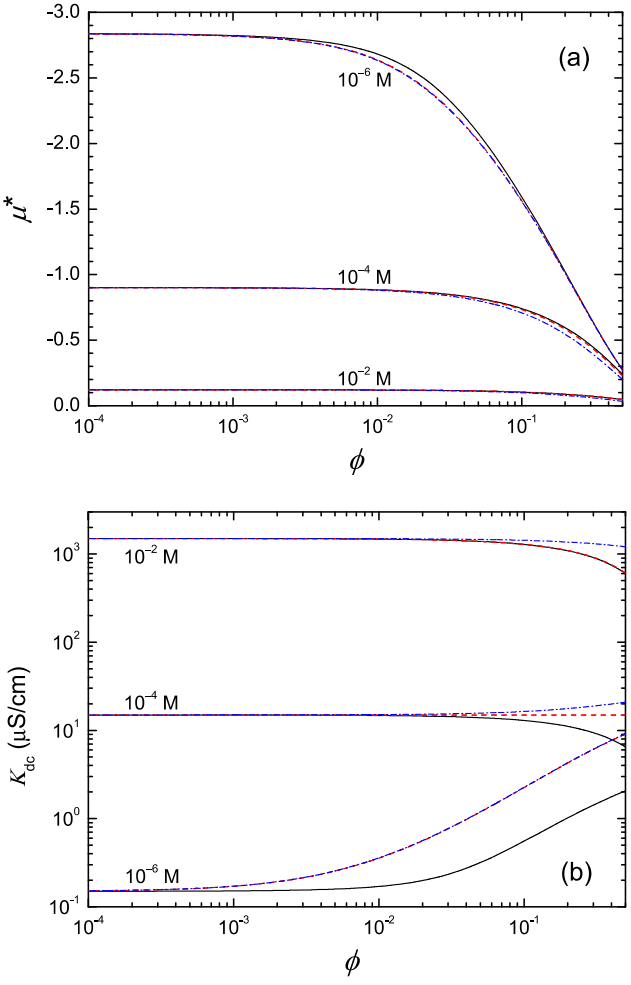

Fig. 1. Dimensionless electrophoretic mobility μ^* (a) and *dc* conductivity K_{dc} (b) as a function of particle volume fraction ϕ for different average KCl concentrations. Surface charge density $\sigma = -0.05$ μC/cm^2, particle radius $a = 250$ nm. ST model: solid dark lines; AC + S(l) model: dashed red lines; AC + S(S) model: dash-dotted blue lines. H^+ as added counterions. Average KCl concentrations: 10^{-6} M, 10^{-4} M, 10^{-2} M. (For interpretation of the references to colour in this figure legend, the reader is referred to the web version of this article.)

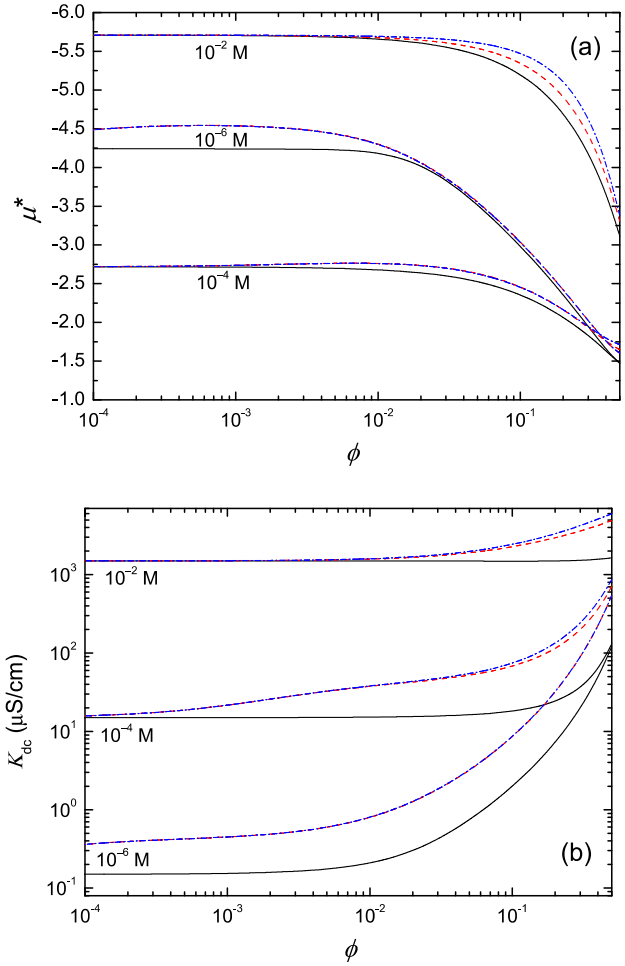

Fig. 2. Same as Fig. 1, but for a surface charge density $\sigma = -25.0$ μC/cm^2.

conditions. The effect is again more notorious in the *dc* conductivity log–log representation in Fig. 1b.

(iv) As salt concentration increases at low volume fractions, ST predictions tend to the AC + S predictions. For such conditions, the much simpler ST model suffices to reach rigorous predictions.

(v) At high salt concentrations and whatever the volume fraction, the ST predictions tend to the AC + S (*l*) ones rather than to the AC + S (*S*) (see mainly Fig. 1b). The reason lies on the fact that the added counterions in the example studied are quite lower in number than those of the salt, and secondly, that the average salt concentration value in the liquid volume is close to the local salt concentration at the outer surface of the cell as no overlapping between double layers occur at such high salt concentrations. Even for the small liquid volume in the cell at high volume fractions, it can be guaranteed that the electro-neutrality is locally attained somewhere inside the cell and extended till the outer surface of the cell, which behaves like the bulk of the ST model.

It is thus confirmed that the ST model is a very close approximation to the AC + S (*l*) model for high average salt concentrations assuming for its $c^{\infty}_{+,-}$ coefficients equal values than the average concentrations of the AC + S (*l*) model, whatever the volume fraction. On the contrary, the ST model seems to deviate from AC + S (*S*) predictions at the same high salt concentration and volume fractions (see upper-right part of Fig. 1b).

On the other hand, as particle surface charge increases, the ST predictions are not as close to those of the more general models AC + S (*l*) or AC + S (*S*). This can be confirmed in Fig. 2a and b for a much higher particle surface charge density, namely, $\sigma = -25.0$ μC/cm^2. While the conductivity predictions in Fig. 2b follow similar trends with volume fraction and salt concentration as those shown in Fig. 1b, the mobility results in Fig. 2a show significant differences with respect to those obtained for low particle charge in Fig. 1a. As salt concentration rises, the mobility first decreases, goes to a minimum and increases again. This pattern is not fulfilled when the surface charge is low and indicates the important effects that mainly relaxation forces play as ionic strength increases, since the surface potential diminishes at increasing salt concentration in Fig. 2a and b. The magnitude of the electric dipole induced by the external field for a given particle charge progressively diminishes as the double layer reduces its width in growing ionic strength conditions. Although the more efficient screening of surface charge as salt concentration increases should lead the mobility to correspondingly decrease, at larger ionic strengths the diminution of the relaxation effect that opposes the particle motion may invert the mobility behavior provoking its increase.

Again, the deviations of the ST model from the AC + S ones are more remarkable for the conductivity results in Fig. 2b. As volume fraction increases for a given salt concentration there is a growing amount of added counterions in a decreasing liquid volume of the cell, and it is precisely the role of the added counterions that is not well managed by the ST model, partly due to the large difference between diffusion coefficients of added counterions, H^+, and K^+ cations from the salt. Hence, unlike the low surface charge case of Fig. 1a and b, the ST model is not a good approximation of more general models at high surface charges and moderate to high volume fractions, although the agreement improves at high salt concentrations and low volume fractions. This is particularly remarkable in the case of dc conductivity (Fig. 2b).

3.2. Model predictions for the electrophoretic mobility

In this section we will compare electrophoretic mobility predictions from three models: ST, AC + S (*l*) and FNEQ (*l*). A similar study might have been done with the models ST, AC + S (*S*) and FNEQ (*S*), but this would be an unnecessary complication for our target of understanding the differences between the general models and the standard one.

First of all, let us make a previous comparison between AC + S (*l*) and FNEQ (*l*) models in Fig. 3. All the differences observed between them for each salt concentration are strictly due to the realistic chemistry of the aqueous solution included only in the FNEQ (*l*) model, as both models correctly allow for the effect of the added counterions and the external salt. We are interested in evaluating the relative role of the ionic content of the realistic aqueous solution (water dissociation and carbon dioxide contamination effects) at increasing salt concentration. In Fig. 3 it is represented the dimensionless electrophoretic mobility of a spherical particle of radius $a = 250$ nm and surface charge density $\sigma = -0.05$ μC/cm^2, in a concentrated suspension, as a function of its particle volume fraction at different average KCl concentrations. Also, their corresponding predictions when no external salt is added to the suspensions are displayed for comparison. Some important conclusions can be extracted from Fig. 3:

(i) In general, the mobility curves show low-volume fraction plateaus followed by decreasing trends at moderate-to-high volume fractions. These behaviors are associated to the independency of particle surface potential with volume fraction in the low volume fraction region for low particle surface charge, and to the effect of decreasing

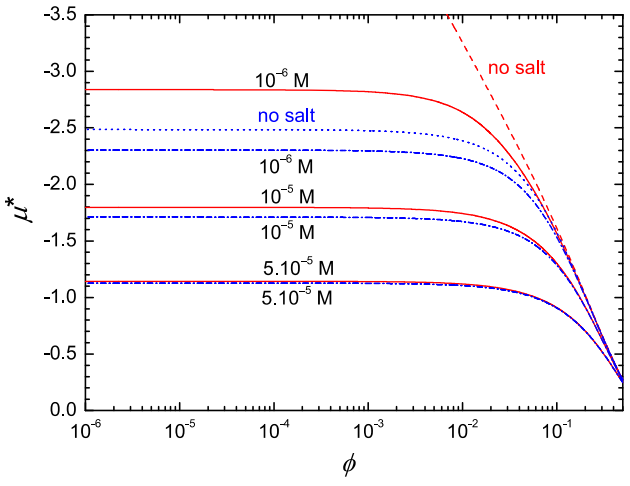

Fig. 3. Dimensionless electrophoretic mobility μ^* as a function of particle volume fraction ϕ for different average KCl concentrations. Surface charge density $\sigma = -0.05$ μC/cm^2, particle radius $a = 250$ nm, H^+ as added counterions. AC + S (l) model: solid red lines; AC + S (l) model, no salt added: dashed red line; FNEQ (l) model: dash-dotted blue lines; FNEQ (l) model, no salt added: dotted blue line. Average KCl concentrations: 10^{-6} M, 10^{-5} M, 5×10^{-5} M. (For interpretation of the references to colour in this figure legend, the reader is referred to the web version of this article.)

particle diffusion length at higher volume fractions. The latter factor in turn leads to larger screening effects on particle surface charge, and correspondingly, to a decrease of the electrophoretic mobility.

(ii) The largest discrepancy observed between models is found at the lowest salt concentration value. The discrepancies rapidly diminish as salt concentration increases. Of course, the relative effect of the realistic aqueous solution is more important the lower the salt concentration when the ions from the salt dissolution do not surpass in concentration those stemming from water dissociation and CO_2 contamination[1]. Note that for a KCl concentration of 5×10^{-5} M, both models predict essentially the same electrophoretic mobility. At such KCl concentration, non-equilibrium effects regarding chemical reactions in solution relative to water and carbonic acid dissociation do not seem to play such an important role as that for low salt concentrations.

(iii) The dimensionless electrophoretic mobility curve when no external salt is added to the suspension shown in Fig. 3 in dashed red line corresponds to the case of a pure salt-free suspension with just its added counterions in solution. Note the remarkable increasing trend of this mobility as volume fraction decreases (−6.84 at a volume fraction $\phi = 10^{-6}$, not depicted in Fig. 3) separating largely from both AC + S (l) and FNEQ (l) predictions even for the case of 10^{-6} M KCl. The consideration of just the realistic chemistry of the aqueous solution is found to reduce the mobility a 63% of its salt free value, yielding a prediction even lower than that of the AC + S (l) for the case of 10^{-6} M KCl. This fact shows the importance of the aqueous realistic solution, which behaves like a low concentrated salt solution, having a clear influence on the mobility. As it was pointed out, a salt concentration of 5×10^{-5} M in the present case is sufficient to completely mask the realistic effects. This result and many others not shown for brevity allow us to conclude that it is not necessary to account for realistic chemistry in most of the cases of moderate-to-high salt concentrations, tending AC + S (l) and FNEQ (l) models to convergent predictions.

Recall that, contrary to the AC + S (l) and FNEQ (l) models, the ST electrokinetic theory does not consider any other ionic species in solution different than those of the salt. A study of the comparison of electrophoretic mobilities according to AC + S (l), FNEQ (l) and ST models can be seen in Figs. 4 and 5. For this study and in order to explore other possible influences of the wide set of parameters affecting the mobility, two different surface charge densities, one moderately low and a rather high one, and a typical particle radius of 100 nm have been chosen. The salt concentration region explored in Figs. 4 and 5 varies from the very low concentration of 10^{-6} M KCl to a moderate one of 10^{-4} M KCl. Note that:

(i) For the lowest surface charge density of −0.1 μC/cm^2 studied in Fig. 4, all the models predict practically the same mobility at the largest salt concentration of 10^{-4} M KCl

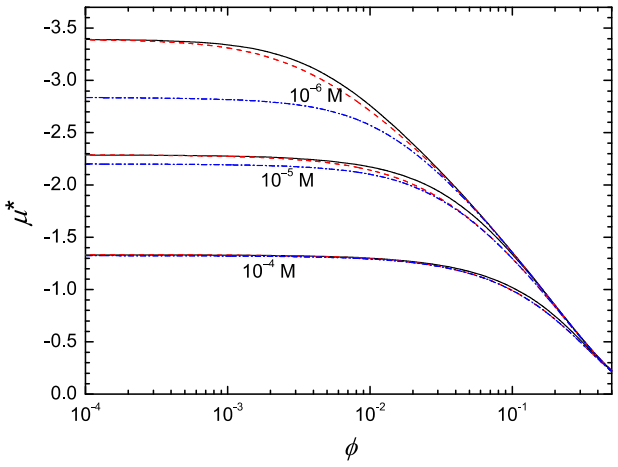

Fig. 4. Dimensionless electrophoretic mobility μ^* as a function of particle volume fraction ϕ for different average KCl concentrations. Surface charge density $\sigma = -0.1$ μC/cm^2, particle radius $a = 100$ nm, H^+ as added counterions. ST model: solid dark lines; AC + S (l) model: dashed red lines; FNEQ (l) model: dash-dotted blue lines. Average KCl concentrations: 10^{-6} M, 10^{-5} M, 10^{-4} M. (For interpretation of the references to colour in this figure legend, the reader is referred to the web version of this article.)

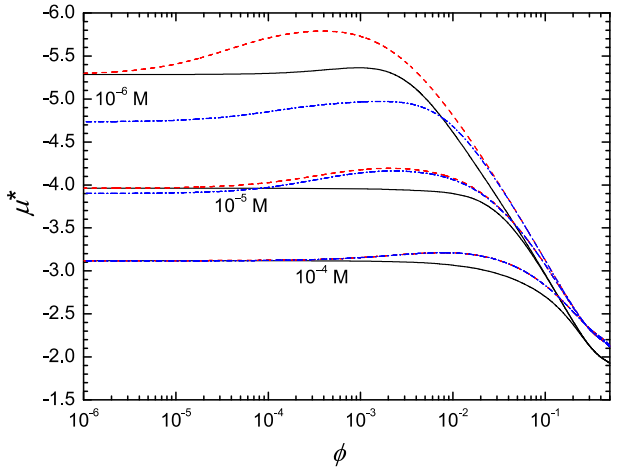

Fig. 5. Same as Fig. 4 but for a particle surface charge density $\sigma = -10.0$ μC/cm^2.

[1] The added counterions are not considered in the discussion because both models correctly take them into account.

whatever the volume fraction. In this case, the ST model suffices to predict results in accordance with those of much more complex models.

(ii) As salt concentration decreases in Fig. 4, the FNEQ (l) model starts to deviate from both AC + S (l) and ST predictions for a wide range of volume fractions (with the exception of the very high ones where the three models tend to coincide again). This fact is more notorious for the lowest salt concentration, but in spite of that, AC + S (l) and ST models continue to give similar predictions with a small discrepancy at intermediate volume fractions, depending on the salt concentration. Of course, ST and AC + S (l) models should tend to coincide as volume fraction goes to the dilute limit because they only differ in the consideration of the added counterions, which are quite low in concentration at such extreme particle dilutions. That is the reason of the common plateau value of AC + S (l) and ST models in such conditions whatever the salt concentration shown in Figs. 4 and 5.

(iii) AC + S (l) and FNEQ (l) models tend to converge as volume fraction increases whatever the salt concentration and particle surface charge density. The effect of the chemical reactions associated with water dissociation and CO_2 contamination in the aqueous solution can be expected to be progressively masked by the increasing amount of added counterions as volume fraction grows at fixed particle charge. On the contrary, AC + S (l) and FNEQ (l) differ considerably at lower volume fractions, especially when the salt concentration is low. In this region the realistic non-equilibrium effects linked to chemical reactions in solution are the most important [22].

(iv) As volume fraction increases, AC + S (l) and ST models start to deviate, reaching a maximum deviation at intermediate volume fractions. The effect is more striking the larger the surface charge density and the lower the salt concentration (see mainly Fig. 5). A large part of such numerical discrepancies are associated with the different ionic mobility of the chosen added counterions, H^+ for the AC + S (l) model, as compared to that of the K^+ cations of the salt. They affect differently, not only the surface potential but also the relaxation and retardation forces acting on the particle, with strong influence on the final electrophoretic mobility. The electric dipole induced on the particle by the electric field has a braking effect on the particle motion for high surface conductance conditions (Dukhin number $Du \gg 1$), known as relaxation effect [24], like those in Fig. 5. Furthermore, larger fluxes of counterions and coions driven by the field in the AC + S (l) case should be expected due to the increasing concentration of ions in the double layer in comparison with the ST model. This might lead to larger retardation forces (viscous stress on the particle by momentum transfer from the double layer ions to the liquid) for the AC + S (l) case. A complicating finding regards the fact that the electrophoretic mobility deviation between AC + S (l) and ST models in the intermediate region of volume fractions increases (see Fig. 5) as surface charge density rises. It seems that the magnitude of the stationary induced dipole moment should decrease in such conditions for the more realistic AC + S (l) model in comparison with the ST one, and therefore, the effect of braking on the electrophoretic mobility should decrease as well. In fact, it has been numerically shown [49] that realistic models predict less significant induced electric dipole moments than those in pure salt-free conditions for the same systems due to the particular distributions of ions in the double layer at the larger ionic strength environments of realistic models. If in our case a similar result were applicable, the relaxation force would be less important and the electrophoretic mobility might increase in spite of the expected enhancement of retardation effects.

In any case, it is important to point out the remarkable approximation of the ST model in predicting electrophoretic mobilities for most of the typical salt concentrations, even as low as 10^{-5} M KCl, at arbitrary volume fractions, provided that the particle surface charge density is low, and also for low volume fractions when the particle surface charge density is high. We believe that our numerical calculations can help in elucidating the question of the importance of neglecting the correct computation of the added counterions and the effects of water dissociation and CO_2 contamination, constraining or supporting its validity from a quantitative point of view. In general, all the effects will be screened by the superior influence of the salt beyond a particular concentration limit. For such cases, the ST model constitutes an easy tool for making rigorous predictions of the electrophoretic mobility without invoking the degree of sophistication of more general models that require extra numerical efforts and larger computational times.

3.3. Predictions of dc electrical conductivity

Finally, we explore the *dc* electrical conductivity of the same suspensions studied in Section 3.2 according to AC + S (l), FNEQ (l) and ST models. Again, we will check under which conditions the simpler ST model may suffice to bring about rigorous predictions. In analogy with the previous study, we will start with a comparison of AC + S (l) and FNEQ (l) models in Fig. 6. Note that:

(i) The conductivity curves show low-volume fraction plateaus followed by increasing trends at moderate-to-high volume fractions. For the AC + S (l) model the initial plateaus are due to the dominance of the salt ions over that of the added counterions at low volume fractions whatever the average salt concentration. The pure salt-free model in dashed red line predicts conductivities quite lower than those of the AC + S (l) model even at the lowest salt concentration of 10^{-6} M KCl in the region of low volume fractions.

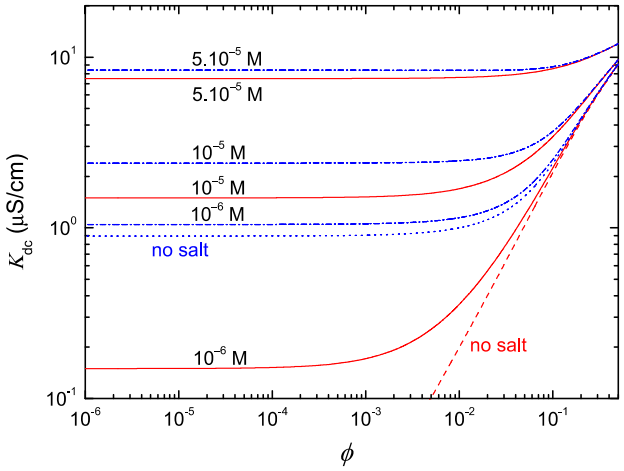

Fig. 6. *dc* conductivity K_{dc} as a function of particle volume fraction for different average KCl concentrations. Surface charge density $\sigma = -0.05$ μC/cm^2, particle radius $a = 250$ nm, H^+ as added counterions. AC + S (l) model: solid red lines; AC + S (l) model, no salt added: dashed red line; FNEQ (l) model: dash-dotted blue lines; FNEQ (l) model, no salt added: dotted blue line. Average KCl concentrations: 10^{-6} M, 10^{-5} M, 5×10^{-5} M. (For interpretation of the references to colour in this figure legend, the reader is referred to the web version of this article.)

(ii) The conductivity plateaus remain until the volume fraction is high enough to increase the conductivity due to the large number of added counterions at every average salt concentration.

(iii) The FNEQ initial conductivity plateaus are firstly due to the ionic species linked to the realistic chemistry of the aqueous solution. As salt concentration increases, the low volume fraction conductivity plateaus augment correspondingly. The behavior as volume fraction increases is similar to the one for the AC + S (l) model already described, as the role of added counterions becomes more relevant the larger the volume fraction. In all cases the AC + S (l) model conductivity predictions are lower than the FNEQ ones for every salt concentration, due to the additional ionic sources in solution of the latter.

(iv) The largest relative discrepancy observed between AC + S (l) and FNEQ (l) will diminish the larger the salt concentration, as it is confirmed in Fig. 6. Note that for the maximum KCl concentration studied of 5×10^{-5} M, both models have not yet attained a full convergence for the majority of particle volume fractions, unlike the corresponding electrophoretic mobilities in Fig. 3. It seems that the conductivity of the suspension is more sensitive to the influence of the realistic aqueous solution than the electrophoretic mobility of a single particle. Thus, it will be unnecessary to account for realistic aqueous chemistry in most of the cases of moderate-to-high salt concentrations, and the much simpler and easier to handle AC + S (l) model would suffice. The question of the incorrect accounting of added counterions by the ST model will be addressed in the following comparison between AC + S (l), FNEQ (l) and ST models.

In Figs. 7 and 8 we show the electrical conductivity of the same suspensions studied in Figs. 4 and 5 according to AC + S (l), FNEQ (l) and ST models. The most remarkable features observed in Figs. 7 and 8 are:

(i) In the case of the lowest surface charge density of -0.1 μC/cm^2 studied in Fig. 7, all the models predict similar values of the conductivity for the largest salt concentration of 10^{-4} M KCl and volume fractions lower than around 10^{-2}. For larger volume fractions, the ST model starts to separate from the rest of model predictions. A similar feature is found in Fig. 8 for the largest surface charge density of -10.0 μC/cm^2 although the onset of volume fraction separating the point of divergence between ST and the rest of models decreases. As previously referred, the salt acquires the main role at such high concentrations, tending to screen the effects relative to the realistic aqueous solution.

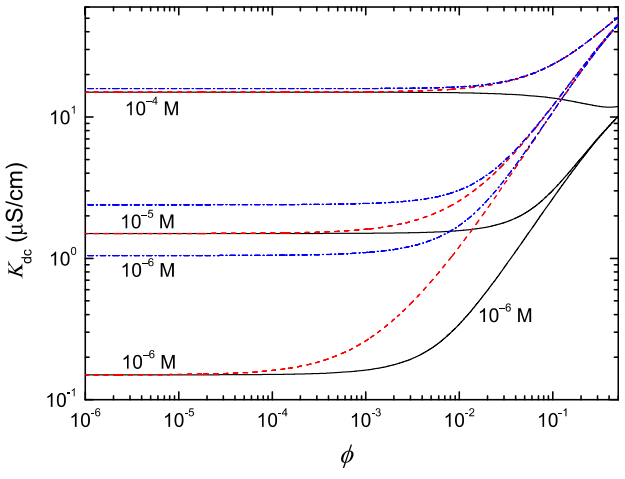

Fig. 7. *dc* conductivity K_{dc} as a function of particle volume fraction for different average KCl concentrations. Surface charge density $\sigma = -0.1$ μC/cm^2, particle radius $a = 100$ nm, H^+ as added counterions. ST model: solid dark lines; AC + S (l) model: dashed red lines; FNEQ (l) model: dash-dotted blue lines. Average KCl concentrations: 10^{-6} M, 10^{-5} M, 10^{-4} M. (For interpretation of the references to colour in this figure legend, the reader is referred to the web version of this article.)

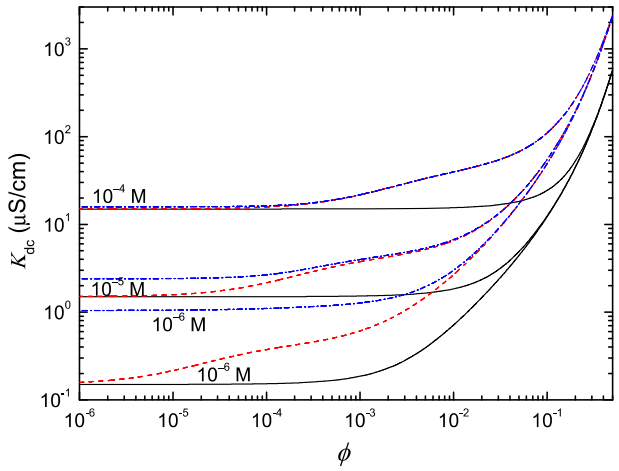

Fig. 8. Same as Fig. 7 but for a particle surface charge density $\sigma = -10.0$ μC/cm^2.

(ii) As volume fraction increases, the added counterions increase their number as well, raising the overall conductivity. This feature is not correctly dealt with by the ST model, considering in addition that the added counterions are H^+ for AC + S (l) and FNEQ (l) models, hence the underestimation of the conductivity by the classical model. This is confirmed when particle charge increases, since a lower volume fraction is necessary to start the deviation of general models from the ST.

(iii) As salt concentration decreases, the FNEQ (l) model remarkably separates from AC + S (l) and ST predictions, showing larger conductivity values. In these conditions, the importance of the realistic contributions of the aqueous solution to the conductivity increases progressively, adding their effects to the rest of charged constituents of the suspension. As in Figs. 4 and 5, AC + S (l) and ST predictions tend to converge at low volume fractions as the role of the added counterions has a limited effect on the conductivity at such low particle concentrations.

(iv) In addition, AC + S (l) and FNEQ (l) models tend to converge as volume fraction increases at fixed salt concentration and particle surface charge density, as clearly shown in Figs. 7 and 8. This is due to the decreasing importance in such conditions of the realistic chemistry of the solution.

(v) Note finally that AC + S (l) predictions for different salt concentrations tend to converge as volume fraction increases at fixed particle surface charge density. The same is observed for FNEQ (l) predictions. Furthermore, both models share the same convergence limit. Instead, ST predictions for different salt concentrations tend to converge at high volume fractions but at a lower convergence limit in comparison with the one of the previous models. These facts mark the onsets of the volume fraction regions where the conductivity starts to be independent of both salt concentration and ionic contributions of the realistic aqueous solution, and begins to be controlled mainly by the charged particles and their added counterions, at least for not very high salt concentrations. The smaller ST conductivity limit can be mostly

related to the smaller ionic mobility coefficient of salt cations in comparison with that of the added counterions, and of course, the neglecting of the specific role of the latter.

4. Conclusions

In this work, we present a general electrokinetic model for concentrated suspensions in aqueous electrolyte solutions. In addition to the ions from a dissolved salt in solution, our calculation features a correct balance of the added counterions released by the particles and also effects associated with the realistic chemistry of the aqueous solution, related to water dissociation and carbon dioxide contamination. Due to the many different couplings that can be established between all the ionic species, some of them linked by non-equilibrium chemical reactions in solution, a unique general model cannot be built which encompasses all possible cases. For this reason, the general model in this work corresponds to the typical situation of a concentrated suspension whose added counterions coincide with one of the aqueous solution. Classically, the dominance of the ions of a dissolved salt over any others in the solution for typical conditions has made the standard model to consider only the ions of the salt and neglect the remaining species. In this work we have tried to make a theoretical analysis about the limits of applicability of the standard (ST) electrokinetic model in aqueous electrolyte solutions. To that aim, the ST model is compared to a more general model that correctly includes the added counterions (AC + S), and to the most general one (FNEQ) that accounts also for a non-equilibrium scenario for chemical reactions in a realistic aqueous solution. In addition, a detailed discussion has been performed regarding the different salt concentration averages in the concentrated suspension referred either to the whole suspension volume (S) or just to its liquid part (l). As a general rule, the presence of salt concentrations larger than around 5×10^{-4} M in solution at low-to-moderate particle volume fractions makes the ST model a real good approximation of more advanced models if the particle surface charge density is low. At lower salt concentrations, ST and AC + S (l) electrokinetic predictions tend to converge because of the minor role the added counterions play in such conditions, but clearly separate from FNEQ predictions due to the realistic effects of the aqueous solution not taken into account in the other two models. Also, for large volume fractions the role of added counterions becomes dominant over those of the salt ions for typical salt concentrations, and general models tend to converge leading to larger deviations from the ST model the larger the particle surface charge density. In summary, classical electrokinetic assumptions have been questioned and information about their applicability has been given. We believe that this work can help in establishing the limits for a correct use of the ST model for concentrated suspensions based on the cell model concept, and assess the conditions under which the more general model cannot be substituted by simpler descriptions of the electrokinetics of concentrated colloidal suspensions.

Acknowledgments

Financial supports for this work by MICINN, Spain (projects FIS2010- 18972, FIS2013-47666-C3-1R, 2R, 3R) and Junta de Andalucía, Spain (project P2012-FQM-694), co-financed with FEDER (European Fund for Regional Development) funds by the EU, are gratefully acknowledged.

Appendix A. Supplementary material

Supplementary data associated with this article can be found, in the online version, at http://dx.doi.org/10.1016/j.jcis.2015.05.023.

References

[1] A.E. Kestell, G.T. DeLorey (Eds.), Nanoparticles: Properties, Classification, Characterization, and Fabrication, Nova Science Publishers Inc, Hauppauge, NY, 2009.
[2] D.A. Giljohann, D.S. Seferos, W.L. Daniel, M.D. Massich, P.C. Patel, C.A. Mirkin, Angew. Chem. Int. Ed. 49 (2010) 3280–3294.
[3] A.S. Dukhin, Z.R. Ulberg, V.I. Karamushka, T.G. Gruzina, Adv. Colloid Interface Sci. 159 (2010) 60–71.
[4] A.V. Delgado, Interfacial Electrokinetics and Electrophoresis, Surfactant Science Series, vol. 106, Marcel Dekker, New York, 2002.
[5] E.K. Zholkovskij, J.H. Masliyah, V.N. Shilov, S. Bhattacharjee, Adv. Colloid Interface Sci. 134–135 (2007) 279–321.
[6] M. Medebach, T. Palberg, J. Chem. Phys. 119 (2003) 3360–3370.
[7] M. Medebach, T. Palberg, Colloids Surf. A: Physicochem. Eng. Aspects 222 (2003) 175–183.
[8] P. Wette, H.J. Schöpe, T. Palberg, Colloids Surf. A: Physicochem. Eng. Aspects 222 (2003) 311–321.
[9] M. Medebach, T. Palberg, J. Phys.: Cond. Mat. 16 (2004) 5653–5658.
[10] T. Palberg, M. Medebach, N. Garbow, M. Evers, A.B. Fontecha, H. Reiber, E. Bartsch, J. Phys.: Cond. Mat. 16 (2004) S4039–S4050.
[11] T. Palberg, J. Phys: Condens. Matt. 26 (2014) 333101. 22 pp.
[12] F. Oosawa, Polyelectrolytes, Marcel Dekker, New York, 1971.
[13] H. Ohshima, J. Colloid Interface Sci. 247 (2002) 18–23.
[14] H. Ohshima, J. Colloid Interface Sci. 248 (2002) 499–503.
[15] H. Ohshima, J. Colloid Interface Sci. 262 (2003) 294–297.
[16] H. Ohshima, J. Colloid Interface Sci. 265 (2003) 422–427.
[17] H. Ohshima, Colloids Surf. A: Physicochem. Eng. Aspects 222 (2003) 207–211.
[18] C.P. Chiang, E. Lee, Y.Y. He, J.P. Hsu, J. Phys. Chem. B 110 (2006) 1490–1498.
[19] F. Carrique, E. Ruiz-Reina, F.J. Arroyo, A.V. Delgado, J. Phys. Chem. B 110 (2006) 18313–18323.
[20] E. Ruiz-Reina, F. Carrique, J. Phys. Chem. C 111 (2007) 141–148.
[21] R. Roa, F. Carrique, E. Ruiz-Reina, Phys. Chem. Chem. Phys. 13 (2011) 19437–19448.
[22] E. Ruiz-Reina, F. Carrique, J. Phys. Chem. B 112 (2008) (1967) 11960–11961.
[23] F. Carrique, E. Ruiz-Reina, L. Lechuga, F.J. Arroyo, A.V. Delgado, Adv. Colloid Interface Sci. 201–201 (2013) 57–67.
[24] S.S. Dukhin, V.N. Shilov, Dielectric Phenomena and the Double Layer in Disperse Systems and Polyelectrolytes, Wiley, New York, 1974.
[25] R.W. O'Brien, L.R. White, J. Chem. Soc., Faraday Trans. 2 (74) (1978) 1607–1626.
[26] R.W. O'Brien, J. Colloid Interface Sci. 81 (1981) 234–248.
[27] C.S. Mangelsdorf, L.R. White, J. Chem. Soc., Faraday Trans. 86 (1990) 2859–2870.
[28] C.S. Mangelsdorf, L.R. White, J. Chem. Soc., Faraday Trans. 94 (1998) 2441–2452.
[29] C.S. Mangelsdorf, L.R. White, J. Chem. Soc., Faraday Trans. 94 (1998) 2583–2593.
[30] P.F. Rider, R.W. O'Brien, J. Fluid Mech. 257 (1993) 607–636.
[31] H. Ohshima, J. Colloid Interface Sci. 195 (1997) 137–148.
[32] A.S. Dukhin, V.N. Shilov, Y.B. Borkovskaya, Langmuir 15 (1999) 3452–3457.
[33] J. Ennis, A.A. Shugai, S.L. Carnie, J. Colloid Interface Sci. 223 (2000) 37–53.
[34] F. Carrique, F.J. Arroyo, M.L. Jiménez, A.V. Delgado, J. Chem. Phys. 118 (2003) 1945–1956.
[35] S. Ahualli, A.V. Delgado, S.J. Miklavcic, L.R. White, Langmuir 22 (2006). 7401-7051.
[36] R. Greenwood, L. Bergström, J. Eur. Ceramic Soc. 17 (1997) 537–548.
[37] S.C. Wang, W.C.J. Wei, J. Am. Ceram. Soc. 84 (2001) 1411–1414.
[38] M. Sjöber, L. Bergström, A. Larsson, E. Sjörstrom, Colloids Surf. A Physicochem. Eng. Aspects 159 (1999) 197–208.
[39] J.L. Amorós, V. Beltrán, V. Sanz, J.C. Jarque, Applied Clay Sci. 49 (2010) 33–43.
[40] R.G. Strickley, Q. Iwata, S. Wu, T.C. Dahl, J. Pharm. Sci. 97 (2008) 1731–1744.
[41] D.M. Kalyon, S. Aktas, Annu. Rev. Chem. Biomol. 5 (2014) 229–254.
[42] S. Alexander, P.M. Chaikin, P. Grant, G.J. Morales, P. Pincus, J. Chem. Phys. 80 (1984) 5776–5781.
[43] L. Belloni, Colloids Surf. A: Physicochem. Eng. Aspects 140 (1998) 227–243.
[44] G.C.L. Wong, L. Pollack, Annu. Rev. Phys. Chem. 61 (2010) 171–189.
[45] V.A. Bloomfield, Biopolymers 44 (1997) 269–282.
[46] D.A.J. Gillespie, J.E. Hallett, E. Oluwapemi, A.F. Che Hamzah, R.M. Richardson, P. Bartlett, Soft Matter 10 (2014) 566–577.
[47] S. Kuwabara, J. Phys. Soc. Jpn. 14 (1959) 527–532.
[48] T. Mori, K. Suma, Y. Sumiyoshi, Y. Endo, J. Chem. Phys. 134 (2011) 044319.
[49] F. Carrique, E. Ruiz-Reina, J. Phys. Chem. B 113 (2009) 8613–8625.